PROCEEDINGS OF SCIENCE

Quasi-degenerate baryon energy states, the Feynman–Hellmann theorem and transition matrix elements

M. Batelaan,[a,1,*] **K. U. Can,**[a] **R. Horsley,**[b,1,*] **Y. Nakamura,**[c] **H. Perlt,**[d] **P. E. L. Rakow,**[e] **G. Schierholz,**[f] **H. Stüben,**[g] **R. D. Young**[a] **and J. M. Zanotti**[a]

[a] *CSSM, Department of Physics, University of Adelaide, Adelaide SA 5005, Australia*
[b] *School of Physics and Astronomy, University of Edinburgh, Edinburgh EH9 3FD, UK*
[c] *RIKEN Center for Computational Science, Kobe, Hyogo 650-0047, Japan*
[d] *Institut für Theoretische Physik, Universität Leipzig, 04109 Leipzig, Germany*
[e] *Theoretical Physics Division, Department of Mathematical Sciences, University of Liverpool, Liverpool L69 3BX, UK*
[f] *Deutsches Elektronen-Synchrotron DESY, Notkestr. 85, 22607 Hamburg, Germany*
[g] *Universität Hamburg, Regionales Rechenzentrum, 20146 Hamburg, Germany*

E-mail: mischa.batelaan@adelaide.edu.au, rhorsley@ph.ed.ac.uk

The standard method for determining matrix elements in lattice QCD requires the computation of three-point correlation functions. This has the disadvantage of requiring two large time separations: one between the hadron source and operator and the other from the operator to the hadron sink. Here we consider an alternative formalism, based on the Dyson expansion leading to the Feynman-Hellmann theorem, which only requires the computation of two-point correlation functions. Both the cases of degenerate energy levels and quasi-degenerate energy levels which correspond to diagonal and transition matrix elements respectively can be considered in this formalism. As an example numerical results for the Sigma to Nucleon vector transition matrix element are presented.

The 39th International Symposium on Lattice Field Theory (Lattice2022),
8-13 August, 2022
Bonn, Germany

[1] For the QCDSF-UKQCD-CSSM Collaborations
[*] Speaker

PoS(LATTICE2022)412

1. Introduction

A major pursuit of lattice QCD is the determination of non-perturbative matrix elements generically given by $\langle H'|\hat{O}|H\rangle$ where H is a hadron such as $H \sim \bar{q}q$ (meson) or $H \sim qqq$ (baryon) and the operator $\hat{O} \sim \bar{q}\gamma q \sim J$ or $\hat{O} \sim FF$ or even more complicated $\hat{O} \sim JJ$. While the usual approach is to compute ratios of 3-point correlation functions to 2-point correlation functions in these talks we will describe an alternative method based on the Feynman–Hellmann theorem, which only involves computing perturbed 2-point correlation functions. In [1] we discussed this for nucleon scattering. However this required degenerate energy states. We shall now describe a generalisation of the Feynman–Hellmann approach from the determination of nucleon matrix elements with degenerate energy states to near-degenerate or 'quasi-degenerate' energy states, [2].

In these talks we shall first discuss the theory behind the Feynman–Hellmann approach via the transfer matrix to a computation of 2-pt correlation functions with particular application to quasi-degenerate states. We employ the Dyson expansion to reduce the problem to a Generalised EigenVector Problem (GEVP) giving avoided energy levels. As examples we first consider N scattering for flavour diagonal matrix elements. However naturally our approach is valid for decay or transition matrix elements, for example the $\Sigma \to N$ transition. (These matrix elements occur in semi-leptonic hyperon decays and provide an alternative approach to determining the CKM matrix element V_{us}, [3].) In both cases we give sketches of avoided energy levels. We then turn to a numerical simulation for the vector current for this transition matrix element, confirming our previous theoretical discussion. Finally we give our conclusions. For more details, see [2].

2. The Feynman–Hellmann approach

In this section we shall give some mathematical details of our Feynman–Hellmann (FH) approach. We employ the Hamiltonian formalism and regard Euclidean time (at least) as continuous. Although our approach is to consider the the 2-point nucleon correlation function, it is valid for all hadrons. We shall make some comments about the introduction of spin later. We have

$$C_{\lambda B'B}(t) = {}_\lambda\langle 0|\hat{\vec{B}}'(0;\vec{p}')\hat{S}(\vec{q})^t\hat{\vec{B}}(0,\vec{0})|0\rangle_\lambda\,, \tag{1}$$

where the source $\hat{\vec{B}}(0,\vec{0})$ is spatial (for simplicity placed at the origin $\vec{0}$) and contains all momenta, while the sink $\tilde{B}'(0;\vec{p}')$ picks out a particular momentum $\vec{p}'$. $\hat{S}$ is the $\vec{q}$-dependent transfer matrix $\hat{S}(\vec{q}) = e^{-\hat{H}(\vec{q})}$ in the presence of a perturbed Hamiltonian

$$\hat{H}(\vec{q}) = \hat{H}_0 - \sum_\alpha \lambda_\alpha \hat{\vec{O}}_\alpha(\vec{q})\,, \tag{2}$$

with

$$\hat{\vec{O}}(\vec{q}) = \int_{\vec{x}} \left(\hat{O}(\vec{x})e^{i\vec{q}\cdot\vec{x}} + \hat{O}^\dagger(\vec{x})e^{-i\vec{q}\cdot\vec{x}}\right)\,. \tag{3}$$

In the large box-size limit, we pick out the ground state of the perturbed Hamiltonian, $|0\rangle_\lambda$ as indicated in eq. (1). At leading order (considered here) we can drop the α index. (At higher orders this is not possible.) Also as we write $\lambda_\alpha = |\lambda_\alpha|\zeta_\alpha$ ($\zeta_\alpha = \pm 1, \pm i$) then any phase can be absorbed into $\hat{O}$ and we can consider positive λ_α only.

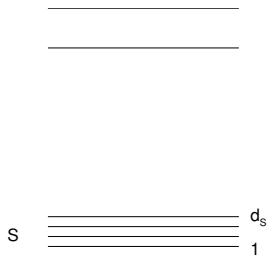

Figure 1: A sketch of the energy levels. The set of quasi-degenerate energy states are denoted by S, labelled from 1 to d_S. These states are well separated from other higher states.

We consider the physical situation with quasi-degenerate energies as shown in Fig. 1, taking the d_S quasi-degenerate states to be well separated from any higher energy states as shown in the figure. Their energies are defined by

$$\hat{H}_0|B_r(\vec{p}_r)\rangle = E_{B_r}(\vec{p}_r)|B_r(\vec{p}_r)\rangle\,, \quad r = 1\,,\ldots,d_S\,, \tag{4}$$

where

$$E_{B_r}(\vec{p}_r) = \bar{E} + \epsilon_r\,, \tag{5}$$

$\bar{E}$ being some typical quasi-degenerate energy (for example their average energy). They are well separated from higher energy states:

$$\hat{H}_0|X(\vec{p}_X)\rangle = E_X(\vec{p}_X)|X(\vec{p}_X)\rangle \quad E_X \gg \bar{E}\,. \tag{6}$$

Practically we thus take the quasi-degenerate states as the lowest energy states.

For the matrix elements corresponding to the quasi-degenerate energy levels in Fig. 1 we have a relation between the various momenta. Using $\hat{O}(\vec{x}) = e^{-i\hat{\vec{p}}\cdot\vec{x}}\,\hat{O}(\vec{0})\,e^{i\hat{\vec{p}}\cdot\vec{x}}$ we soon see that

$$\langle B(\vec{p}_r)|\hat{\tilde{O}}(\vec{q})|B(\vec{p}_s)\rangle = \langle B_r(\vec{p}_r)|\hat{O}(\vec{0})|B_s(\vec{p}_s)\rangle\,\delta_{\vec{p}_r,\vec{p}_s+\vec{q}} + \langle B(\vec{p}_r)|\hat{O}^\dagger(\vec{0})|B(\vec{p}_s)\rangle\,\delta_{\vec{p}_r,\vec{p}_s-\vec{q}}\,. \tag{7}$$

So matrix elements step up or down in $\vec{q} \neq \vec{0}$

$$\vec{p}_r = \vec{p}_s + \vec{q}\,, \quad \text{or} \quad \vec{p}_r = \vec{p}_s - \vec{q}\,, \tag{8}$$

i.e. momentum conservation. (For $\vec{q} \to \vec{0}$ the states coalesce, a special case.) We see immediately that diagonal matrix elements vanish. So (quasi)-degenerate states have to mix with one other and we must consider degenerate perturbation theory. We expect that each step up or down corresponds to another order in λ as can be seen from the forthcoming Dyson expansion. So for example the $O(\lambda^2)$ term gives Compton-like amplitudes $\sim \langle \ldots|\hat{O}_\alpha\hat{O}_\beta|\ldots\rangle$. In this case both step up and step down are now possible: $\vec{p}_s \to \vec{p}_s \pm \vec{q} \to \vec{p}_s$ which are relevant for the forward Compton amplitude in e.g. DIS which is considered elsewhere, [4–6].

Now insert two complete sets of unperturbed states[1]

$$\sum\!\!\!\!\!\!\int_{X(\vec{p}_X)} |X(\vec{p}_X)\rangle\,\langle X(\vec{p}_X)| \equiv \sum_r \underbrace{|B_r(\vec{p}_r)\rangle\langle B_r(\vec{p}_r)|}_{\text{of interest}} + \sum\!\!\!\!\!\!\int_{E_X \gg \bar{E}} \underbrace{|X(\vec{p}_X)\rangle\,\langle X(\vec{p}_X)|}_{\text{higher states}} = \hat{1}\,, \tag{9}$$

[1]We use the (lattice) normalisation $\langle X|X\rangle = 1$. To convert to other normalisations use $|X\rangle \to |X\rangle/\sqrt{\langle X|X\rangle}$ and $|0\rangle \to |0\rangle$. In particular for the standard relativistic normalisation we have $\langle X|X\rangle = 2E_X$ (used in eq. (39)).

before and after $\hat{S}^t$ to give

$$C_{\lambda B'B}(t) = \sum\!\!\!\!\!\!\int_{X(\vec{p}_X)} \sum\!\!\!\!\!\!\int_{Y(\vec{p}_Y)} {}_\lambda\langle 0|\hat{\bar{B}}'(\vec{p}')|X(\vec{p}_X)\rangle \, \langle X(\vec{p}_X)|\hat{S}_\lambda(\vec{q})^t|Y(\vec{p}_Y)\rangle \, \langle Y(\vec{p}_Y)|\hat{\bar{B}}(\vec{0})|0\rangle_\lambda \,. \quad (10)$$

Time dependent perturbation theory via the Dyson Series iterates the operator identity

$$e^{-(\hat{H}_0-\lambda_\alpha\hat{\bar{O}}_\alpha)t} \;=\; e^{-\hat{H}_0 t} + \lambda_\alpha \int_0^t dt' \, e^{-\hat{H}_0(t-t')} \, \hat{\bar{O}}_\alpha \, e^{-(\hat{H}_0-\cancel{\lambda_\beta\hat{\bar{O}}_\beta})t'} \,, \quad (11)$$

where at leading order we simply drop the perturbation under the integral as indicated. As mentioned before the $O(\lambda_\alpha\lambda_\beta)$ term would give Compton like amplitudes $\sim \langle \ldots|\hat{O}_\alpha\hat{O}_\beta|\ldots\rangle$. Considering the possible pieces separately from eq. (9) gives finally the result, [2],

$$C_{\lambda B'B}(t) = \sum_{i=1}^{d_S} w^{(i)}_{B'} \bar{w}^{(i)}_{B} \, e^{-E^{(i)}_\lambda t} + \ldots \,, \quad (12)$$

with perturbed energies

$$E^{(i)}_\lambda = \bar{E} - \mu^{(i)} \,, \quad i = 1, \ldots, d_S \,, \quad (13)$$

where $\mu^{(i)}$ are the eigenvalues[2] of the $d_S \times d_S$ Hermitian matrix D_{rs} defined by

$$D_{rs} = -\epsilon_r\delta_{rs} + \lambda\langle B_r(\vec{p}_r)|\hat{\bar{O}}(\vec{q})|B_s(\vec{p}_s)\rangle \,. \quad (14)$$

Furthermore in eq. (12) we have

$$w^{(i)}_{B'} = \sum_{r=1}^{d_s} Z^{B'}_r e^{(i)}_r \,, \quad \text{and} \quad \bar{w}^{(i)}_{B} = \sum_{s=1}^{d_s} \bar{Z}^{B}_s e^{(i)*}_s \,, \quad (15)$$

where $\vec{e}^{(i)}$, $i = 1, \ldots, d_s$ are the d_s eigenvectors of D_{rs} and the wavefunctions are given by

$$Z^{B'}_r = {}_\lambda\langle 0|\hat{\bar{B}}'(\vec{p}')|B_r(\vec{p}_r)\rangle_\lambda \,, \quad \text{and} \quad \bar{Z}^{B}_s = {}_\lambda\langle B_s(\vec{p}_s)|\hat{\bar{B}}(\vec{0})|0\rangle_\lambda \,, \quad (16)$$

where the states $|B_s(\vec{p}_s)\rangle_\lambda$ are defined by

$$|B_s(\vec{p}_s)\rangle_\lambda = |B_s(\vec{p}_s)\rangle + \lambda \sum\!\!\!\!\!\!\int_{E_Y \gg \bar{E}} |Y(\vec{p}_Y)\rangle \, \frac{\langle Y(\vec{p}_Y)|\hat{\bar{O}}(\vec{q})|B_s(\vec{p}_s)\rangle}{E_Y - E_{B_s}} \,. \quad (17)$$

We see that there is a factorisation where the unwanted $|Y\rangle$ states have been absorbed into a time independent renormalisation of the wavefunction.

So from eq. (12) we see that the problem is now 'reduced' to a GEVP or Generalised Eigen-Vector Problem, [7, 8], which can be applied to determine the energy eigenvalues $E^{(i)}_\lambda$ as described in section 5.

In principle this means that we can extend the computation to include lower energy states $|Z\rangle$ in the spectrum, with $E_Z \ll \bar{E}$, i.e. again well separated from the quasi-energy states. If there are such states present in eq. (9) then we need to avoid any transitions between these states and either the

[2] D_{rs} is decomposed as $D_{rs} = \sum_{i=1}^{d_S} \mu^{(i)} e^{(i)}_r e^{(i)*}_s$.

quasi-degenerate states or the higher energy states, as these will have a term $\sim e^{-E_Z t}$ and hence will be the leading term in eq. (12). This can be achieved by a possible mixture of vanishing overlaps with these states, vanishing matrix elements and regarding them as extra terms in the GEVP. We do not consider this lower energy case further here.

Finally note that the above result is true for general source and sink operators. If we are able to set $\hat{B}'$ and $\hat{B}$ 'close' to $\hat{B}_r$ and $\hat{B}_s$ respectively then the above expressions simplify and we have

$$w_r^{(i)} = Z_r e_r^{(i)}\,, \quad \text{and} \quad \bar{w}_s^{(i)} = \bar{Z}_s e_s^{(i)*}\,. \tag{18}$$

3. Examples

Let us consider a $d_S = 2$-fold case: $r, s = 1, 2$. Then due to the step up or down in $\vec{q}$ for the matrix element we must have

$$\langle B_r(\vec{p}_r)|\hat{\hat{O}}(\vec{q})|B_s(\vec{p}_s)\rangle = \begin{pmatrix} 0 & a^* \\ a & 0 \end{pmatrix}_{rs}\,, \quad \text{where} \quad a = \langle B_2(\vec{p}_2)|\hat{O}(\vec{0})|B_1(\vec{p}_1)\rangle\,. \tag{19}$$

Diagonalising $D_{rs}(\vec{p},\vec{q})$ in eq. (14) gives upon solving the quadratic equation the eigenvalues $\mu_\pm$ giving energies

$$E_\lambda^{(\pm)} = \bar{E} - \mu_\pm = \frac{1}{2}(E_2 + E_1) \mp \frac{1}{2}\Delta E_\lambda\,, \tag{20}$$

with

$$\Delta E_\lambda = E_\lambda^{(-)} - E_\lambda^{(+)} = \sqrt{(E_2 - E_1)^2 + 4\lambda^2|a|^2}\,. \tag{21}$$

A flavour diagonal matrix element is given from nucleon scattering where we have

$$O(\vec{x}) \sim (\bar{u}\gamma u)(\vec{x}) - (\bar{d}\gamma d)(\vec{x})\,, \quad \text{and} \quad \underbrace{|B_1(\vec{p}_1)\rangle = |N(\vec{p})\rangle}_{E_{B_1}(\vec{p}_1)\equiv E_N(\vec{p})=\bar{E}+\epsilon_1}\,, \quad \underbrace{|B_2(\vec{p}_2)\rangle = |N(\vec{p}+\vec{q})\rangle}_{E_{B_2}(\vec{p}_2)\equiv E_N(\vec{p}+\vec{q})=\bar{E}+\epsilon_2}\,. \tag{22}$$

In general we have quasi-degenerate energy states, but it is easy to choose $\vec{p}$ and $\vec{q}$ so the energies are degenerate $E_N(\vec{p}+\vec{q}) = E_N(\vec{p})$, [1]. (A similar situation occurs if we consider $E_N(\vec{p}-\vec{q})$ instead.) For flavour transition matrix elements for example $\Sigma(sdd) \to N(udd)$ decay we have

$$O(\vec{x}) \sim (\bar{u}\gamma s)(\vec{x})\,, \quad \text{and} \quad \underbrace{|B_1(\vec{p}_1)\rangle = |\Sigma(\vec{p})\rangle}_{E_{B_1}(\vec{p}_1)\equiv E_\Sigma(\vec{p})=\bar{E}+\epsilon_1}\,, \quad \underbrace{|B_2(\vec{p}_2)\rangle = |N(\vec{p}+\vec{q})\rangle}_{E_{B_2}(\vec{p}_2)\equiv E_N(\vec{p}+\vec{q})=\bar{E}+\epsilon_2}\,. \tag{23}$$

As $M_\Sigma \neq M_N$ then we now usually have quasi-degenerate energy states. Both cases (diagonal and transition matrix elements) thus have a similar structure.

We now illustrate these results with a series of (exaggerated) 1-dimensional sketches. For nucleon scattering, eq. (22), we have the situation depicted in Fig. 2. We focus on the degeneracy when $E_N(p) = E_N(p+q)$ at $p = -q/2$ where in addition $\epsilon_1 = 0 = \epsilon_2$. When the free case (left panel of Fig. 2) becomes the interacting case (right panel of Fig. 2) we have the phenomenon of 'avoided energy level crossing' when the energy levels do not cross. The sketch curves are based on

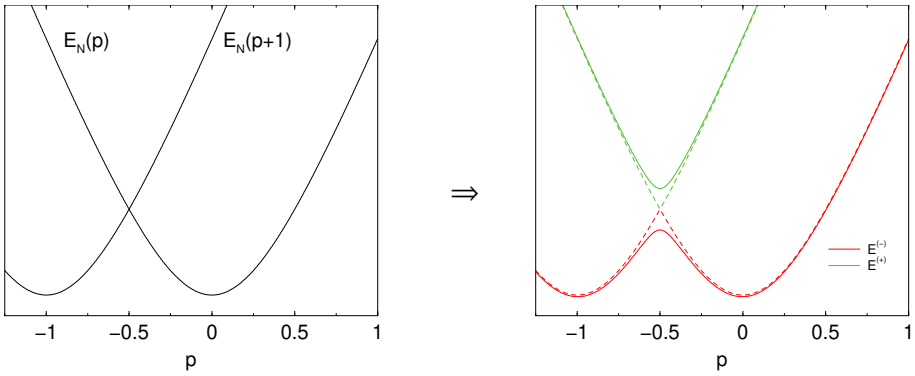

Figure 2: Left panel: Plotting p versus E_N for the free case when we have quasi-degenerate energies taking units where $q = 1$ at $p \approx -1/2$. Right panel: The interacting case showing 'avoided energy levels'. The $\lambda \to 0$ or free case is shown as dashed lines.

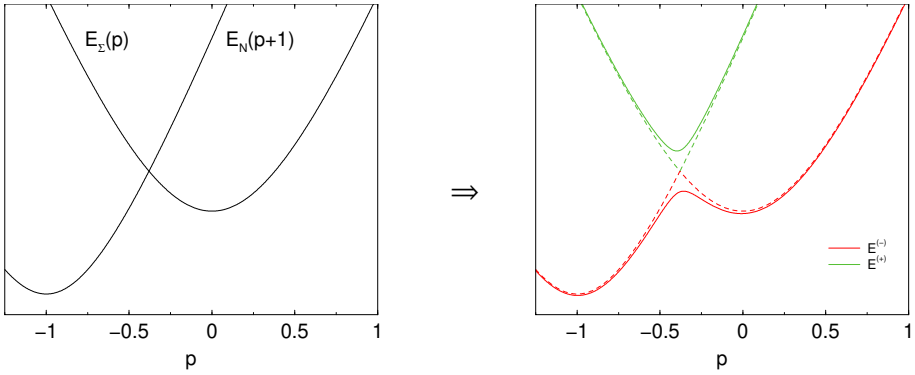

Figure 3: Left panel: The free case when we have quasi-degenerate energies again taking units where $q = 1$. Right panel: The interacting case showing 'avoided energy levels'.

previously derived formulae for $E^{(+)}$, $E^{(-)}$ in eq. (20) and occur because in eq. (21) the square-root is always positive. Again note that a similar situation arises when $E_N(p) = E_N(p-q)$ at $p = q/2$ (not shown in the sketch). A similar situation occurs for $\Sigma \to N$ decay as illustrated in Fig. 3. Again we have a degeneracy: $E_\Sigma(p) = E_N(p+q)$ which is now shifted slightly to smaller p, as indicated in the figure.

The eigenvectors $e_r^{(\pm)}$ are given by

$$e_r^{(\pm)} = N^{(\pm)} \begin{pmatrix} \lambda|a| \\ \kappa_\pm \frac{a}{|a|} \end{pmatrix}_r , \qquad \text{with} \qquad \kappa_\pm = \tfrac{1}{2}(E_1 - E_2) \pm \tfrac{1}{2}\Delta E \,, \tag{24}$$

where the $N^{(\pm)}$ normalisation factor is chosen so that $|e_1^{(\pm)}|^2 + |e_2^{(\pm)}|^2 = 1$. As $a = |a|\zeta_a$ ($\zeta_a = \pm 1, \pm i$) then as expected any possible phase of the matrix element is contained in the eigenvectors, the energy must be real. Note that the components of the eigenvectors are related: $e_2^{(-)} = -e_1^{(+)}\zeta_a$ and $e_2^{(+)} = e_1^{(-)}\zeta_a$. We sketch their behaviour in Fig. 4. Shown are sketches of eq. (24) for $e_1^{(-)\,2}$ and $e_2^{(-)\,2}$ against p both for the free and interacting case corresponding for the eigenvalues for $\Sigma \to N$ shown in Fig. 3. While in the free case the components of $\vec{e}^{(\pm)}$ remain constant (left panel) for the interacting case (right panel) they flip as the momentum p changes.

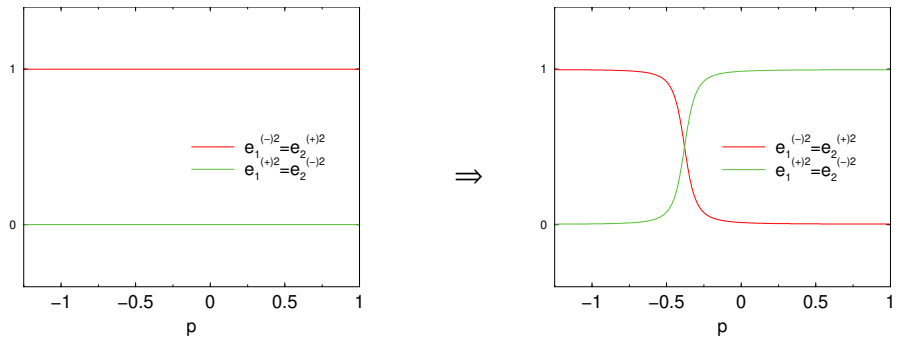

Figure 4: Left panel: The free case where we have plotted $e_1^{(-)\,2}$ and $e_2^{(-)\,2}$ against p, again taking units where $q = 1$. Right panel: The interacting case showing the change of state.

4. Incorporating the spin index

We now make a few comments on how the spin index is incorporated into the formalism. Further details are given in [2]. We have the replacement

$$|B_r(\vec{p}_r)\rangle \to |B_r(\vec{p}_r, \sigma_r)\rangle\,, \tag{25}$$

where $\sigma_r = \pm$ is the spin index. Hence the D matrix is doubled in size $\sigma_r r = +1, -1, \ldots + d_S, -d_S$ i.e. we now have a $2d_S \times 2d_S$ matrix. However due to Kramers' degeneracy theorem the energy states corresponding to $|B_r(\vec{p}_r, \sigma_r)\rangle$, are doubly degenerate, so we still have d_S energy eigenvalues. We could continue as before with this enlarged matrix. However it is advantageous to try to keep as close as possible to the previous results. We can achieve this by writing the overlaps as

$$\begin{aligned} {}_\lambda\langle 0|\hat{B}_{r\,\alpha}(\vec{0})|B_r(\vec{p}_r, \sigma_r)\rangle_\lambda &= Z_r\, u_\alpha^{(r)}(\vec{p}_r, \sigma_r) + \ldots\,, \\ {}_\lambda\langle B_s(\vec{p}_s, \sigma_s)|\hat{\bar{B}}_{s\,\beta}(\vec{0})|0\rangle_\lambda &= \bar{Z}_s\, \bar{u}_\beta^{(s)}(\vec{p}_s, \sigma_s) + \ldots\,, \end{aligned} \tag{26}$$

where Z_r and $\bar{Z}_s$ are taken as scalars. Although the states here are the perturbed states, rather than the unperturbed states, we expect the effect of the perturbation to be small as from eq. (17) the $O(\lambda)$ terms involve overlaps such as $\langle 0|\hat{B}_r|Y\rangle$ or $\langle X|\hat{B}_r|B_r\rangle$ which vanish or are small due to the orthogonality of the spectrum. Furthermore, although we could consider the Dirac indices as a GEVP it is convenient to sum over them with some matrix, Γ. Presently we only numerically consider the unpolarised case with $\Gamma^{\text{unpol}} = (1 + \gamma_4)/2$ so

$$C_{\lambda rs}(t) = \text{tr}\,\Gamma^{\text{unpol}} C_{\lambda B_r B_s}(t)\,. \tag{27}$$

This reduces D to the previous $d_S \times d_S$ matrix as in eq. (14) and leads to the replacement in eq. (19) of $a \to (a_{++} + a_{--})/2$ where the indices are the spin components. So effectively this is the same result as before, we are just averaging over the spins. So this gives finally

$$C_{\lambda rs}(t) = \sum_{i=1}^{d_S} w_r^{(i)} \bar{w}_s^{(i)} e^{-E_\lambda^{(i)} t}\,. \tag{28}$$

Alternatively an explicit form factor decomposition of the matrix elements (for all possible γ matrices) shows that different spin components of matrix elements are related to each other. The

upshot is that for previous examples in section 3 for $d_S = 2$ we first make the replacement

$$a \to \begin{pmatrix} a_{++} & a_{+-} \\ a_{-+} & a_{--} \end{pmatrix}, \tag{29}$$

with $a_{--} = \eta a^*_{++}$, $a_{-+} = -\eta a^*_{+-}$ ($\eta = \pm$ depending on the matrix element considered) and in the previous results we replace $|a| \to |\det a|^{1/2}$ where $|\det a| = |a_{++}|^2 + |a_{+-}|^2$. As we pick out either a_{++} or a_{+-} this is equivalent to the previous procedure.

5. A lattice application for transition matrix elements

As an example of this formalism, we shall now consider in more detail how the previous results can be applied to the $\Sigma \to N$ transition matrix element. We first discuss the necessary modifications to the action and the fermion inversion procedure before considering the specific numerical results.

To apply the results of section 3 we need to consider the action

$$S = S_g + \int_x (\bar{u}, \bar{s}) \begin{pmatrix} D_u & -\lambda\mathcal{T} \\ -\lambda\mathcal{T}' & D_s \end{pmatrix} \begin{pmatrix} u \\ s \end{pmatrix} + \int_x \bar{d}\, D_d\, d\,, \tag{30}$$

where S_g is the gluon action and the fermionic piece is explicitly given. (For simplicity we absorb any clover terms into the Ds.) We take the u and d quarks as mass degenerate $m_u = m_d \equiv m_l$, with a common mass m_l. For $\mathcal{T}$ we take the general local expression

$$\mathcal{T}(x, y; \vec{q}) = \gamma\, e^{i\vec{q}\cdot\vec{x}}\, \delta_{x,y}\,, \tag{31}$$

and for γ_5-hermiticity for the matrix in eq. (30) we need $\mathcal{T}' = \gamma_5 \mathcal{T}^\dagger \gamma_5$.

From the action in eq. (30) we see that we now need to invert a larger matrix to find the propagator for the various correlation functions. Although possible directly, we have found it advantageous to consider it as a 2×2 block matrix and invert that. This leads to

$$\begin{aligned} G^{(uu)} &= (1 - \lambda^2 D_u^{-1} \mathcal{T} D_s^{-1} \gamma_5 \mathcal{T}^\dagger \gamma_5)^{-1} D_u^{-1}\,, \\ G^{(ss)} &= (1 - \lambda^2 D_s^{-1} \gamma_5 \mathcal{T}^\dagger \gamma_5 D_u^{-1} \mathcal{T})^{-1} D_s^{-1}\,, \end{aligned} \tag{32}$$

and

$$\begin{aligned} G^{(us)} &= \lambda D_u^{-1} \mathcal{T} G^{(ss)}\,, \\ G^{(su)} &= \lambda D_s^{-1} \gamma_5 \mathcal{T}^\dagger \gamma_5 G^{(uu)}\,. \end{aligned} \tag{33}$$

The problem with eq. (32) is that it involves an inversion within an inversion, which computationally would be very expensive. However for λ small (the case considered here) it is sufficient to expand to a low order in λ, especially as the expansion parameter is λ^2. To build the Green's functions we use $\delta_{\vec{x},\vec{0}}\delta_{t,0}$ as the initial source, and build the chain using the previously calculated object as the new source. This has the advantage of producing the Green's function and hence correlation function matrix

$$C_{\lambda rs}(t) = \begin{pmatrix} C_{\lambda\Sigma\Sigma}(t) & C_{\lambda\Sigma N}(t) \\ C_{\lambda N\Sigma}(t) & C_{\lambda NN}(t) \end{pmatrix}_{rs}, \tag{34}$$

as a continuous function of λ rather than needing a separate evaluation for each value of λ chosen.

We now apply the GEVP (Generalised EigenValue Problem) to the 2×2 correlator matrix $C_\lambda(t)$, eq. (34). The variation of the method we use here, [9], is first to determine the left $v^{(i)}$ and right $u^{(i)}$ eigenvectors by considering the correlation matrix at times t_0 and $t_0 + \Delta t_0$. These can be combined with the correlator matrix to construct a new correlation function

$$C_\lambda^{(i)}(t) = v^{(i)\,\dagger} C_\lambda(t) u^{(i)}\,, \quad i = \pm\,. \tag{35}$$

These two correlators $C_\lambda^{(i)}(t)$, $i = \pm$ represent the two GEVP energy eigenstates of the system $\propto e^{-E_\lambda^{(i)} t}$ which of course includes the perturbation to the action. To relate this to the transition form factors, we require the energy splitting between these two states and so from eqs. (20), (21) we construct the ratio of the correlators

$$R_\lambda(t) = \frac{C_\lambda^{(-)}(t)}{C_\lambda^{(+)}(t)} \overset{t\gg 0}{\propto} e^{-\Delta E_\lambda t}\,, \tag{36}$$

which in the large Euclidean time limit will behave like a single-exponential function and will show up in the effective energy as a plateau region. We thus use this effective energy to pick out a suitable plateau region and then fit a single-exponential function to the ratio. The two important parameters of the GEVP calculation are t_0 and Δt_0. Optimally the time range from t_0 and $t_0 + \Delta t_0$ needs to be in a region where the ground state is saturated but the signal-to-noise ratio is still sufficiently high to exclude any effects from higher states. Finally we note that using eqs. (18), (28) means that

$$v_r^{(i)} = \frac{N^{(i)}}{Z_r}\, e_r^{(i)}\,, \quad \text{and} \quad u_s^{(i)} = \frac{\bar{N}^{(i)}}{\bar{Z}_s}\, e_s^{(i)}\,, \tag{37}$$

where $N^{(i)}$ and $\bar{N}^{(i)}$ are normalisation constants. Essentially $v_r^{(i)*}$ measures the component of B_r in the i^{th} eigenvector and similarly for $u_s^{(i)}$ and $\bar{B}_s$.

6. Lattice results

While the above discussion is general, we now consider the concrete case of the vector matrix element V_4 for $\Sigma \to N$ where the Σ is stationary, i.e. $\vec{p}_1 = \vec{0}$ and $\vec{p}_2 = \vec{q}$ in eq. (23). Then the (Euclidean) momentum transfer is given in this case by[3]

$$q = (i(M_\Sigma - E_N(\vec{q})), \vec{q})\,, \quad \text{or} \quad Q^2 = -(M_\Sigma - E_N(\vec{q}))^2 + \vec{q}^{\,2}\,. \tag{38}$$

Thus from eq. (21) we must compute

$$\Delta E_\lambda = \sqrt{(E_N - M_\Sigma)^2 + 4\lambda^2 \left(\frac{\langle N(\vec{q}) | \bar{u}\gamma_4 s | \Sigma(\vec{0}) \rangle}{(2E_N)(2M_\Sigma)} \right)^2}\,. \tag{39}$$

[3]Note that we have adopted the convention that q is positive for a scattering process where for the scattered baryon the momentum q is added to the initial baryon momentum. This is opposite to the semi-leptonic case, where the lepton and neutrino carry momentum q.

Numerical simulations have been performed using $N_f = 2+1$ $O(a)$ improved clover Wilson fermions [10] at $\beta = 5.50$ and $(\kappa_l, \kappa_s) = (0.121040, 0.120620)$ on a $N_s^3 \times N_t = 32^3 \times 64$ lattice. More definitions and details are given in [11]. We just mention here that our strategy is to keep the average bare quark mass constant from the $SU(3)$ flavour symmetric point. This situation corresponds to a lattice spacing of $a \sim 0.074\,\text{fm} \sim 1/(2.67\,\text{GeV})$ leading to a pion mass of $\sim 330\,\text{MeV}$. Errors given in the following are primarily statistical (using $\sim O(500)$ configurations) using a bootstrap method.

Clearly we need to keep the energy states close to each other. As spatial momentum on the lattice is discretised and given in each direction in steps of $2\pi/N_s$, which is coarse on this lattice size. To obtain a finer energy level separation we use twisted boundary conditions, [12, 13], in the y-direction and set $\vec{q} = (0, \theta_2/N_s, 0)$ and take 6 values of the twist parameter θ_2 such that in lattice units $\vec{q}^2$ runs from 0 (run #1) to ~ 0.05 (run #6), so that $Q^2 \sim -0.01\,\text{GeV}^2$ to $\sim 0.35\,\text{GeV}^2$.

Using each of these momentum values we calculate the correlation function matrix in eq. (34) up to order $O(\lambda^4)$ in the expansion of eqs. (32) and (33). Since the multiplication with λ occurs after the fermion matrix inversions, we are able to construct the correlation function matrix for a large number of λ values in the range $\lambda = (0, \ldots, 0.05)$. After solving the GEVP for each of these matrices we construct the ratio in eq. (36). The effective energy of this ratio is shown in Fig. 5 for

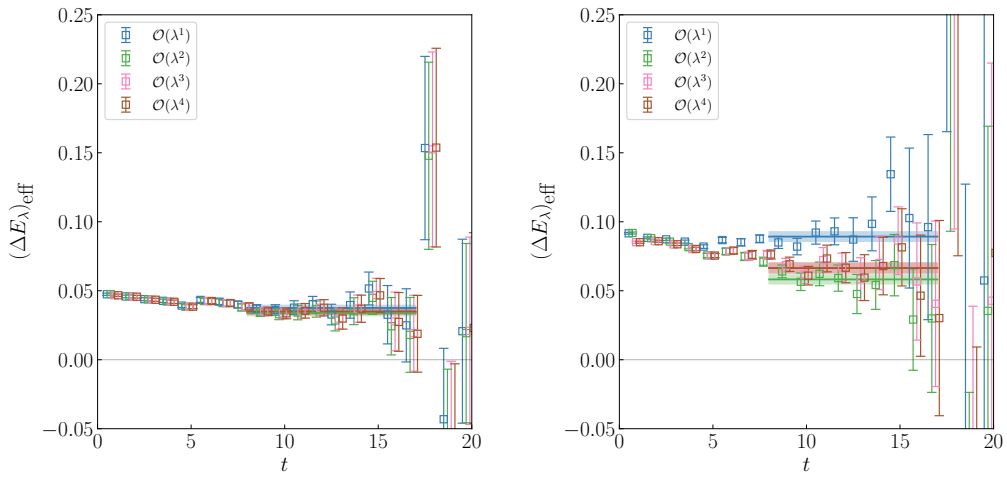

Figure 5: LH panel: $(\Delta E_\lambda)_{\text{eff}} = -\ln(R_\lambda(t+1)/R_\lambda(t))$ versus t for $\lambda = 0.025$ at $O(\lambda)$, $O(\lambda^2)$, $O(\lambda^3)$ and $O(\lambda^4)$ for run #5. RH panel: similarly for $\lambda = 0.05$. The points are slightly offset for visibility.

run #5 at two different λ values. The right hand plot in this figure also shows the effect of the higher order corrections at $\lambda = 0.05$.

Figure 6 shows the dependence of the energy shift on λ for each of the four orders in the expansion for run #1 and run #5. Once again we can see that as λ increases the lower orders of the expansion start to deviate and higher order corrections are required. The expansion seems to hold up better for run #5 where the energy gap between the unperturbed states is minimized. However even for run #1, there is a sufficiently large λ range available to extract the matrix element.

The matrix element can then be extracted by using eq. (39), the result of which is shown in Fig. 7. We also show the results of a three-point function calculation on the same configurations, there is good agreement between the two methods.

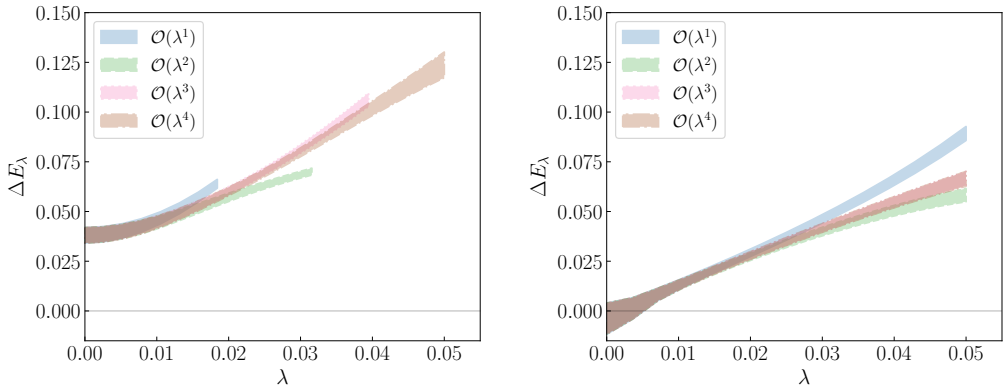

Figure 6: LH panel: The λ-dependence for run #1 for ΔE_λ. The numerical results for each order in λ ($O(\lambda)$, $O(\lambda^2)$, $O(\lambda^3)$ and $O(\lambda^4)$) are given as bands. RH panel: Similarly for run #5.

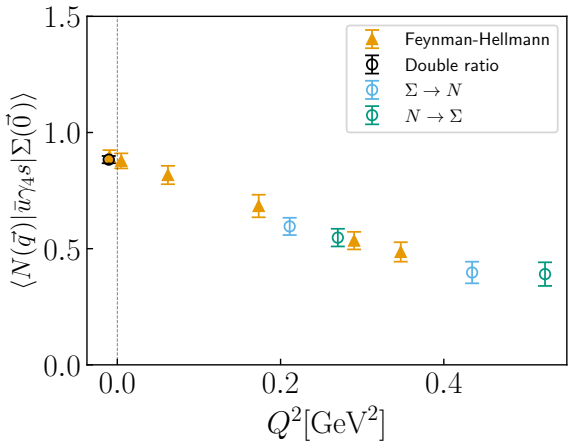

Figure 7: The renormalised transition matrix element as a function of Q^2 from the Feynman-Hellmann method (triangles) and from the three-point function method (circles). (Z_V is taken from [14].)

7. Conclusions

The Feynman-Hellmann approach has been shown here to be a viable alternative to the conventional three-point function method for calculating matrix elements. The Feynman-Hellmann approach allows for a simpler analysis of excited state contributions as the resulting correlator has the same structure as a two-point function. This allows for the application of the many established techniques for analysing two-point correlation functions. To extend this method to transition matrix elements has required reformulating it for quasi-degenerate states and using partially twisted boundary conditions to achieve these quasi-degeneracies. The extention also allows for the inclusion of higher orders in the λ expansion which has allowed us to extend the range of λ which can be used. We have shown that this method can produce results with good agreement to the three-point function method for the $\Sigma \to N$ transition for Q^2 values -0.01 GeV^2 to 0.35 GeV^2. Further details are given in [2].

Acknowledgements

The numerical configuration generation (using the BQCD lattice QCD program [15])) and data analysis (using the Chroma software library [16]) was carried out on the DiRAC Blue Gene Q and Extreme Scaling (EPCC, Edinburgh, UK) and Data Intensive (Cambridge, UK) services, the GCS supercomputers JUQUEEN and JUWELS (NIC, Jülich, Germany) and resources provided by HLRN (The North-German Supercomputer Alliance), the NCI National Facility in Canberra, Australia (supported by the Australian Commonwealth Government) and the Phoenix HPC service (University of Adelaide). RH is supported by STFC through grant ST/P000630/1. HP is supported by DFG Grant No. PE 2792/2-1. PELR is supported in part by the STFC under contract ST/G00062X/1. GS is supported by DFG Grant No. SCHI 179/8-1. RDY and JMZ are supported by the Australian Research Council grant DP190100297. For the purpose of open access, the authors have applied a Creative Commons Attribution (CC BY) licence to any author accepted manuscript version arising from this submission.

References

[1] A. J. Chambers *et al.*, Phys. Rev. D **96** (2017) 114509, [arXiv:1702.01513 [hep-lat]].

[2] M. Batelaan *et al.*, [QCDSF-UKQCD-CSSM Collaborations], in preparation.

[3] N. Cabibbo *et al.*, Phys. Rev. Lett. **92** (2004) 251803, [arXiv:hep-ph/0307214].

[4] A. J. Chambers *et al.*, Phys. Rev. Lett. **118** (2017) 242001, [arXiv:1703.01153 [hep-lat]].

[5] K. U. Can *et al.*, Phys. Rev. D **102** (2020) 114505, [arXiv:2007.01523 [hep-lat]].

[6] K. U. Can, PoS **LATTICE2022** (2023) 237, [arXiv:2212.09197 [hep-lat]].

[7] M. Lüscher *et al.*, Nucl. Phys. B **339** (1990) 222.

[8] B. Blossier *et al.*, JHEP **04** (2009) 094, [arXiv:0902.1265 [hep-lat]].

[9] B. J. Owen *et al.*, Phys. Lett. B **723** (2013) 217, [arXiv:1212.4668 [hep-lat]].

[10] N. Cundy *et al.*, Phys. Rev. D **79** (2009) 094507, [arXiv:0901.3302 [hep-lat]].

[11] W. Bietenholz *et al.*, Phys. Rev. D **84** (2011) 054509, [arXiv:1102.5300 [hep-lat]].

[12] P. F. Bedaque, Phys. Lett. B **593** (2004) 82, [arXiv:nucl-th/0402051 [nucl-th]].

[13] J. M. Flynn *et al.*, JHEP **05** (2007) 016, [arXiv:hep-lat/0703005 [hep-lat]].

[14] J. M. Bickerton *et al.*, Phys. Rev. D **100** (2019) 114516, [arXiv:1909.02521 [hep-lat]].

[15] T. R. Haar *et al.*, EPJ Web Conf. **175** (2018) 14011, [arXiv:1711.03836 [hep-lat]].

[16] R. G. Edwards *et al.*, Nucl. Phys. B Proc. Suppl. **140** (2005) 832, [arXiv:hep-lat/0409003].